Selection Combining Scheme over Non-identically Distributed Fisher-Snedecor $\mathcal{F}$ Fading Channels

Hussien Al-Hmood, *Member, IEEE,* and H. S. Al-Raweshidy, *Senior Member, IEEE*

***Abstract*—In this paper, the performance of the selection combining (SC) scheme over independent and non-identically distributed (i.n.i.d.) Fisher-Snedecor $\mathcal{F}$ fading channels is analysed. Accordingly, the probability density function (PDF) and the moment generating function (MGF) of the maximum of i.n.i.d. Fisher-Snedecor $\mathcal{F}$ variates are derived first. Based on these statistics, the exact expression and the asymptotic behaviour at high average signal-to-noise ratio value of the average bit error probability (ABEP), the normalised average channel capacity (ACC), and the average area under the receiver operating characteristics curve (AUC) of the energy detection based spectrum sensing with i.n.i.d. SC diversity receivers are provided. To validate our analysis, the numerical results are compared with the Monte Carlo simulations.**

***Index Terms*—Selection combining, Fisher-Snedecor $\mathcal{F}$ fading, average error probability, channel capacity, energy detection.**

I. Introduction

SELECTION combining (SC) diversity reception has been widely used in the literature to improve the performance of wireless communications systems. This is because it has low implementation complexity in comparison with the maximal ratio combining (MRC) where the branch with a high signal-to-noise ratio (SNR) is selected among many branches [1].

The probability density function (PDF), the cumulative distribution function (CDF), and the moment generating function (MGF), of the maximum of random variables (RVs) are employed to analyse the performance of the SC scheme [2]-[5]. For instance, the behaviour of SC receivers over independent and non-identically distributed (i.n.i.d.) generalized-K (K_G) fading was investigated in [2]. The average bit error probability (ABEP) of SC with i.n.i.d. branches over $\kappa-\mu$ shadowed fading was derived in [3]. In [4], the statistics of the maximum of $\eta-\mu$/gamma RVs were provided with applications to the average channel capacity (ACC). The average area under the receiver operating characteristics (ROC) curve (AUC) of energy detection (ED) with SC branches was presented in [5].

Recently, the Fisher-Snedecor $\mathcal{F}$ fading has been proposed as a composite of Nakagami-m and inverse Nakagami-m distributions to model the device-to-device (D2D) fading channel at 5.8 GHz in both indoor and outdoor environments [6], [7]. In contrast to the K_G fading, the statistics of the Fisher-Snedecor $\mathcal{F}$ distribution are expressed in simple elementary functions. Furthermore, it includes Nakagami-m, Rayleigh, and one-sided Gaussian as special cases. The Fisher-Snedecor $\mathcal{F}$ fading can be utilised for both the line-of-sight (LoS) and the non-LoS (NLoS) communications scenarios with better fitting to the empirical measurements than the K_G. Consequently, the ABEP of the MRC was analysed in [8] using the PDF of the sum of i.n.i.d. Fisher-Snedecor $\mathcal{F}$ variates. The behaviour of an ED with square law selection (SLS) in i.n.i.d. Fisher-Snedecor $\mathcal{F}$ fading was studied in [9]. The distribution of the ratio of products of Fisher-Snedecor $\mathcal{F}$ RVs was presented in [10].

To the best of authors' knowledge, no work has been yet devoted in the literature to derive the statistical properties of the maximum of i.n.i.d. Fisher-Snedecor $\mathcal{F}$ variates. Motivated by this, our main contributions in this paper are twofold.

- We derive the exact and the asymptotic expressions at high average SNR value of the PDF and the MGF of the maximum of i.n.i.d. Fisher-Snedecor $\mathcal{F}$ RVs.
- Capitalising on the above, the performance of the ABEP, the ACC, and the average AUC of ED with i.n.i.d. SC diversity receivers are analysed. To this end, mathematically tractable closed-form expressions are obtained.

II. Fisher-Snedecor $\mathcal{F}$ Fading Channel

The CDF of the instantaneous SNR at ith receiver, γ_i over Fisher-Snedecor $\mathcal{F}$ fading is expressed as [7, eq. (12)]

$$F_{\gamma_i}(\gamma)=\frac{\Xi_i^{m_i}\gamma^{m_i}}{m_iB(m_i,m_{s_i})}{}_2F_1(m_i+m_{s_i},m_i;1+m_i;-\Xi_i\gamma)\overset{(a_1)}{=}\Phi_i\gamma^{m_i}H_{2,2}^{1,2}\left[\Xi_i\gamma\middle|\begin{matrix}(1-m_i-m_{s_i},1),(1-m_i,1)\\(0,1),(-m_i,1)\end{matrix}\right] \tag{1}$$

where $\Xi_i=\frac{m_i}{(m_{s_i}-1)\bar{\gamma}_i}$, $\Phi_i=\frac{\Xi_i^{m_i}}{\Gamma(m_i)\Gamma(m_{s_i})}$, m_i is the real extension of the number of multipath clusters, $m_{s_i}>1$ stands for the shadowing severity parameter, $B(.,.)$ is the beta function [11, eq. (8.380.1)], ${}_2F_1(.,.;.;.)$ is the Gauss hypergeometric function [11, eq. (9.14.1)], and $H_{p,q}^{m,n}[.]$ is the Fox's H-function (FHF) defined in [12, eq. (1.2)]. Step (a_1) is developed by applying the identities [12, eq. (1.132)] and [11, eq. (8.384.1)/ eq. (8.331.1)].

III. Maximum I.N.I.D. Fisher-Snedecor $\mathcal{F}$ Variates

Proposition 1: Let all RVs, $\gamma_i\sim\mathcal{F}(m_i,m_{s_i},\bar{\gamma}_i)$ for $i\in\{1,\cdots,L\}$ where L is the number of the variates, follow i.n.i.d. Fisher-Snedecor $\mathcal{F}$ distribution. Thus, the PDF of $\gamma=\max\{\gamma_1,\cdots,\gamma_L\}$ is derived as in (2) shown at the top of the next page. In (2), $\Phi=\prod_{i=1}^{L}\Phi_i$, $\Omega=\sum_{i=1}^{L}m_i$ and

Manuscript received June 6, 2020; xxxxxx xxxxx xxxxx xxxxx.

Hussien Al-Hmood is with the Electrical and Electronics Engineering Department, College of Engineering, University of Thi-Qar, Iraq, e-mails: Hussien.Al-Hmood@brunel.ac.uk, Hussien.Al-Hmood@utq.edu.iq.

H. S. Al-Raweshidy is with the Electronic and Computer Engineering Department, College of Engineering, Design and Physical Sciences, Brunel University London, UK, e-mail: Hamed.Al-Raweshidy@brunel.ac.uk.

$$f_\gamma(\gamma)=\Phi\gamma^{\Omega-1}H_{1,1:[2,2]_{i=1:L}}^{0,1:[1,2]_{i=1:L}}\left[\Xi_1\gamma,\cdots,\Xi_L\gamma\middle|\begin{matrix}(-\Omega;\{1\}_{i=1:L})\\(1-\Omega;\{1\}_{i=1:L})\end{matrix}\middle|\begin{matrix}[(1-m_i-m_{s_i},1),(1-m_i,1)]_{i=1:L}\\[(0,1),(-m_i,1)]_{i=1:L}\end{matrix}\right] \tag{2}$$

$$\mathcal{M}_\gamma(s)=\frac{\Phi}{s^\Omega}H_{1,0:[2,2]_{i=1:L}}^{0,1:[1,2]_{i=1:L}}\left[\frac{\Xi_1}{s},\cdots,\frac{\Xi_L}{s}\middle|(-\Omega;\{1\}_{i=1:L})\middle|\begin{matrix}[(1-m_i-m_{s_i},1),(1-m_i,1)]_{i=1:L}\\[(0,1),(-m_i,1)]_{i=1:L}\end{matrix}\right] \tag{9}$$

$$P_e=\frac{\Phi}{2\sqrt{\pi}\rho^\Omega}H_{1,0:[2,2]_{i=1:L}}^{0,1:[1,2]_{i=1:L}}\left[\frac{\Xi_1}{\rho},\cdots,\frac{\Xi_L}{\rho}\middle|(0.5-\Omega;\{1\}_{i=1:L})\middle|\begin{matrix}[(1-m_i-m_{s_i},1),(1-m_i,1)]_{i=1:L}\\[(0,1),(-m_i,1)]_{i=1:L}\end{matrix}\right] \tag{14}$$

$H_{p,q:[p_i,q_i]_{i=1:L}}^{m,n:[m_i,n_i]_{i=1:L}}[.]$ is the extended generalised bivariate Fox's H-function (EGBFHF) [12, eq. (A.1)] that can be evaluated by using an efficient MATLAB code of [13].

Proof: The CDF of the maximum i.n.i.d. variates can be computed via inserting (1) in $F_\gamma(\gamma)=\prod_{i=1}^L F_{\gamma_i}(\gamma)$ [4, eq. (12)]. Accordingly, we have

$$F_\gamma(\gamma)=\Phi\prod_{i=1}^L\gamma^{m_i}H_{2,2}^{1,2}\left[\Xi_i\gamma\middle|\begin{matrix}(1-m_i-m_{s_i},1),(1-m_i,1)\\(0,1),(-m_i,1)\end{matrix}\right] \tag{4}$$

Recalling the definition of the FHF [12, eq. (1.2)], (4) can be expressed in multiple Barnes-type closed contours as

$$F_\gamma(\gamma)=\frac{\Phi}{(2\pi j)^L}\int_{\mathbb{U}_1}\cdots\int_{\mathbb{U}_L}\left\{\prod_{i=1}^L\Gamma(u_i)\Gamma(m_i+m_{s_i}-u_i)\frac{\Gamma(m_i-u_i)}{\Gamma(1+m_i-u_i)}\Xi_i^{-u_i}\right\}\gamma^{\Omega-\sum_{i=1}^L u_i}du_1\cdots du_L \tag{5}$$

where $j=\sqrt{-1}$ and $\mathbb{U}_i$ is the ith suitable contour in the u-plane from $\sigma_i-j\infty$ to $\sigma_i+j\infty$ with σ_i is a constant value.

Differentiating (5) with respect to γ to obtain $f_\gamma(\gamma)$, i.e., $f_\gamma(\gamma)=dF_\gamma(\gamma)/d\gamma$ and then invoking the identity $\Gamma(1+x)=x\Gamma(x)$ [11, eq. (8.331.1)]. Thus, this yields

$$f_\gamma(\gamma)=\frac{\Phi}{(2\pi j)^L}\int_{\mathbb{U}_1}\cdots\int_{\mathbb{U}_L}\left\{\prod_{i=1}^L\Gamma(u_i)\Gamma(m_i+m_{s_i}-u_i)\frac{\Gamma(m_i-u_i)}{\Gamma(1+m_i-u_i)}\Xi_i^{-u_i}\right\}\frac{\Gamma(1+\Omega-\sum_{i=1}^L u_i)}{\Gamma(\Omega-\sum_{i=1}^L u_i)}\gamma^{\Omega-\sum_{i=1}^L u_i-1}du_1\cdots du_L \tag{6}$$

With the help of [12, eq. (A.1)], (6) can be written in exact closed-form expression as in (2) which finishes the proof. ■

Since ${}_2F_1(.,.;.;.)$ of (1) tends to unity when $\bar{\gamma}_i\to\infty$, the asymptotic of the CDF, $F_\gamma^{\text{Asy}}(\gamma)$, can be expressed as

$$F_\gamma^{\text{Asy}}(\gamma)\approx\prod_{i=1}^L\frac{\Xi_i^{m_i}}{m_iB(m_i,m_{s_i})}\gamma^{m_i} \tag{7}$$

Making use of $f_\gamma^{\text{Asy}}(\gamma)=dF_\gamma^{\text{Asy}}(\gamma)/d\gamma$, the PDF at high average SNR value is obtained as

$$f_\gamma^{\text{Asy}}(\gamma)\approx\Omega\left(\prod_{i=1}^L\frac{\Xi_i^{m_i}}{m_iB(m_i,m_{s_i})}\right)\gamma^{\Omega-1} \tag{8}$$

Proposition 2: The MGF of γ, $\mathcal{M}_\gamma(s)$, is provided in (9) as shown at the top of this page.

Proof: The MGF can be calculated by plugging (5) in $\mathcal{M}_\gamma(s)=s\mathcal{L}\{F_\gamma(\gamma);-s\}$ where $\mathcal{L}\{.\}$ represents the Laplace transform operation. Hence, we have

$$\mathcal{M}_\gamma(s)=\frac{\Phi}{(2\pi j)^L}\int_{\mathbb{U}_1}\cdots\int_{\mathbb{U}_L}\left\{\prod_{i=1}^L\Gamma(u_i)\Gamma(m_i+m_{s_i}-u_i)\frac{\Gamma(m_i-u_i)}{\Gamma(1+m_i-u_i)}\Xi_i^{-u_i}\right\}s\mathcal{L}\{\gamma^{\Omega-\sum_{i=1}^L u_i};-s\}du_1\cdots du_L \tag{10}$$

Invoking [11, eq. (3.381.4)] to compute the Laplace transform of (10) and recalling [12, eq. (A.1)], (9) is deduced. ■

Using (7) and following the same steps of the Proposition 2, the asymptotic of the MGF, $\mathcal{M}_\gamma^{\text{Asy}}(s)$, is given by

$$\mathcal{M}_\gamma^{\text{Asy}}(s)\approx\left(\prod_{i=1}^L\frac{\Xi_i^{m_i}}{m_iB(m_i,m_{s_i})}\right)\frac{\Gamma(1+\Omega)}{s^\Omega} \tag{11}$$

IV. Performance Analysis of SC Scheme

A. Average Bit Error Probability

The ABEP can be evaluated by [1, eq. (9.11)]

$$P_e=\frac{1}{\pi}\int_0^{\frac{\pi}{2}}\mathcal{M}_\gamma\left(\frac{\rho}{\sin^2\theta}\right)d\theta. \tag{12}$$

where $\rho=0.5$, $\rho=1$, and $\rho=0.715$ for coherent binary frequency shift keying (BFSK), binary phase shift keying (BPSK), and BFSK with minimum correlation, respectively.

Substituting (9) into (12) and employing [12, eq. (A.1)] and $x=\sin^2\theta$, the following inner integral is obtained

$$\int_0^1\frac{x^{\Omega-\sum_{i=1}^L u_i-\frac{1}{2}}}{\sqrt{1-x}}dx\overset{(a_2)}{=}\frac{\Gamma(\frac{1}{2})\Gamma\left(\frac{1}{2}+\Omega-\sum_{i=1}^L u_i\right)}{\Gamma\left(1+\Omega-\sum_{i=1}^L u_i\right)} \tag{13}$$

where (a_2) follows [11, eq. (3.191.3)/ eq. (8.384.1)].

Next, plugging the result of (13) and the remaining parts of (9) in (12) and invoking [12, eq. (A.1)], P_e is yielded as given in (14) at the top of this page.

Inserting (11) in (12) and using $x=\sin^2\theta$ as well as following the same procedure of (13), the asymptotic of the ABEP at high average SNR regime, P_e^{Asy}, is expressed as

$$P_e^{\text{Asy}}\approx\left(\prod_{i=1}^L\frac{\Xi_i^{m_i}}{m_iB(m_i,m_{s_i})}\right)\frac{\Gamma(0.5+\Omega)}{2\sqrt{\pi}\rho^\Omega} \tag{15}$$

After substituting $\Xi_i=\frac{m_i}{(m_{s_i}-1)\bar{\gamma}_i}$ into (15) and approximating the result to be $P_e^{\text{Asy}}\approx\bar{\gamma}^{-G_d}$ where G_d denotes the

$$\bar{C} = \frac{\Phi}{\ln 2} H_{1,1:[2,2]_{i=1:L}}^{1,1:[1,2]_{i=1:L}} \left[\Xi_1, \cdots, \Xi_L \middle| \begin{matrix} (1-\Omega;\{1\}_{i=1:L}) \\ (1-\Omega;\{1\}_{i=1:L}) \end{matrix} \middle| \begin{matrix} [(1-m_i-m_{s_i},1),(1-m_i,1)]_{i=1:L} \\ [(0,1),(-m_i,1)]_{i=1:L} \end{matrix} \right] \tag{18}$$

$$\begin{aligned} \bar{A} =& 1 - \Phi \sum_{k=0}^{u-1} \sum_{l=0}^{k} \binom{k+u-1}{k-l} \frac{1}{2^{k-\Omega+u} l!} \\ & \times H_{2,1:[2,2]_{i=1:L}}^{0,2:[1,2]_{i=1:L}} \left[2\Xi_1, \cdots, 2\Xi_L \middle| \begin{matrix} (-\Omega,\{1\}_{i=1:L}),(1-l-\Omega,\{1\}_{i=1:L}) \\ (1-\Omega,\{1\}_{i=1:L}) \end{matrix} \middle| \begin{matrix} [(1-m_i-m_{s_i},1),(1-m_i,1)]_{i=1:L} \\ [(0,1),(-m_1,1)]_{i=1:L} \end{matrix} \right] \end{aligned} \tag{23}$$

diversity order, one can observe that G_d is proportional to L and m_i, i.e., $P_e^{\text{Asy}} \approx \prod_{i=1}^{L} \bar{\gamma}_i^{-m_i}$, whereas for independent and identically distributed (i.i.d.) branches, $G_d = Lm$. These observations are consistent with [6] in which $G_d = m$ for $L = 1$.

B. Average Channel Capacity

The normalised ACC, $\bar{C}$, can be computed by [7, eq. (20)]

$$\bar{C} = \frac{1}{\ln 2} \int_0^{\infty} \ln(1+\gamma) f_\gamma(\gamma) d\gamma \tag{16}$$

Plugging (6) in (16), we have the following inner integral

$$\begin{aligned} & \int_0^{\infty} \gamma^{\Omega - \sum_{i=1}^{L} u_i - 1} \ln(1+\gamma) d\gamma \\ & \quad \overset{(a_3)}{=} \frac{\Gamma(1-\Omega+\sum_{i=1}^{L} u_i)[\Gamma(\Omega-\sum_{i=1}^{L} u_i)]^2}{\Gamma(1+\Omega-\sum_{i=1}^{L} u_i)} \end{aligned} \tag{17}$$

where (a_3) obtains after using [11, eq. (4.293.10)] and recalling [11, eq. (8.334.3)/ eq. (8.331.1)].

Substituting the result of (17) and the remaining terms of (6) into (16), $\bar{C}$ is yielded as in (18) at the top of this page.

Inserting (11) in [4, eq. (27)], the asymptotic of the normalised ACC at $\bar{\gamma}_i \to \infty$, $\bar{C}^{\text{Asy}}$, is derived as

$$\bar{C}^{\text{Asy}} \approx \sum_{l=1}^{M} \frac{w_l}{x_l \ln 2} \left[1 - \left(\prod_{i=1}^{L} \frac{\Xi_i^{m_i}}{m_i B(m_i, m_{s_i})} \right) \frac{\Gamma(1+\Omega)}{x_l^{\Omega}} \right] \tag{19}$$

where M is the number of terms for the Gaussian-Laguerre integration whereas x_l and w_l are the abscissas and the weight factors, respectively [16].

It is obvious that G_d of (19) is proportional to L and m_i for i.n.i.d. case, whereas $G_d = Lm$ for identical receivers.

C. Average AUC of Energy Detection Based-Spectrum Sensing

The AUC is a single figure of merit that evaluates the area under the ROC curve. Hence, the AUC is used in the analysis of the ED when the ROC curve doesn't give a clear insight into the behaviour of the system.

The average AUC, $\bar{A}$, can be calculated by [9, eq. (36)]

$$\bar{A} = \int_0^{\infty} A(\gamma) f_\gamma(\gamma) d\gamma \tag{20}$$

where $A(\gamma)$ is given as [9, eq. (35)]

$$A(\gamma) = 1 - \sum_{k=0}^{u-1} \sum_{l=0}^{k} \binom{k+u-1}{k-l} \frac{1}{2^{k+l+u} l!} \gamma^l e^{-\frac{l}{2}} \tag{21}$$

where $u = TB$ is the time (T)-bandwidth (B) product and $\binom{b}{a}$ denotes the binomial coefficient.

After plugging (21) and (6) in (20) and invoking $\int_0^{\infty} f_\gamma(\gamma) d\gamma \triangleq 1$, the following inner integral is obtained

$$\begin{aligned} & \int_0^{\infty} \gamma^{l+\Omega-\sum_{i=1}^{L} u_i - 1} e^{-\frac{l}{2}} d\gamma \\ & \quad \overset{(a_4)}{=} 2^{l+\Omega-\sum_{i=1}^{L} u_i} \Gamma\left(l + \Omega - \sum_{i=1}^{L} u_i \right) \end{aligned} \tag{22}$$

where (a_4) arises after utilising [11, eq. (3.381.4)].

Substituting the result of (22) as well as the remaining parts of (6) and (21) into (20), we have a closed-form expression of $\bar{A}$ as shown in (23) at the top of this page.

Inserting (8) and (21) in (20) and with the aid of [11, eq. (3.381.4)], the asymptotic analysis of the AUC at high average SNR regime, $\bar{A}^{\text{Asy}}$, is derived as

$$\begin{aligned} \bar{A}^{\text{Asy}} \approx & \left(\prod_{i=1}^{L} \frac{\Xi_i^{m_i}}{m_i B(m_i, m_{s_i})} \right) \\ & \times \left[1 - \sum_{k=0}^{u-1} \sum_{l=0}^{k} \binom{k+u-1}{k-l} \frac{\Gamma(l+\Omega)}{2^{k-\Omega+u} l!} \right] \end{aligned} \tag{24}$$

Similar to (15) and (19), the diversity order, G_d, of (24) which is for arbitrary distributed branches, is proportional to L and m_i, whereas $G_d = Lm$ for i.i.d. case.

V. Analytical and Simulation Results

In this section, to validate our analysis, the Monte Carlo simulations that are obtained via generating 10^7 realizations for each RV are compared with the analytical results. The Fisher-Snedecor $\mathcal{F}$ fading channel of SC scheme was generated by the product of independent variates that were obtained via the inverse CDF of the inverse Nakagami-m and Nakagami-m distributions. Three scenarios of the shadowing impact, which are heavy, moderate, and light are studied by using $m_s = 1.5$, $m_s = 5$ and $m_s = 50$, respectively.

Figs. 1 and 2 illustrate the ABEP for BPSK and the normalised ACC with $M = 15$ for single receiver, dual, and triple SC branches over i.n.i.d. Fisher-Snedecor $\mathcal{F}$ fading channels. As anticipated, the performance becomes better when the SC scheme is employed and monotonically improves with the increasing in the number of the diversity branches. This is because the received average SNR of SC with $L = 3$ is higher than the no-diversity, i.e. $L = 1$, and $L = 2$ cases. For example, in Fig. 1, at fixed $\bar{\gamma} = 7$ dB and $m_s = 1.5$, the

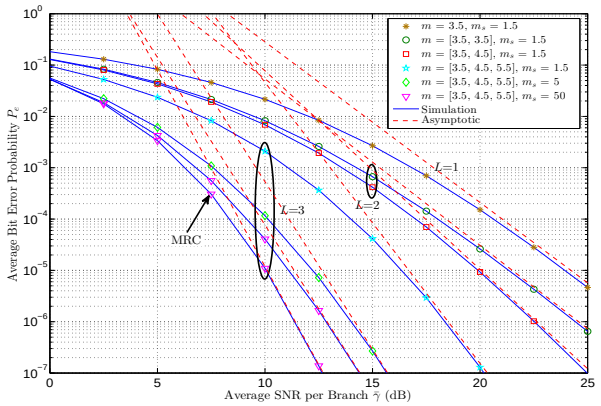

Fig. 1. ABEP for BPSK of SC scheme with i.n.i.d. branches.

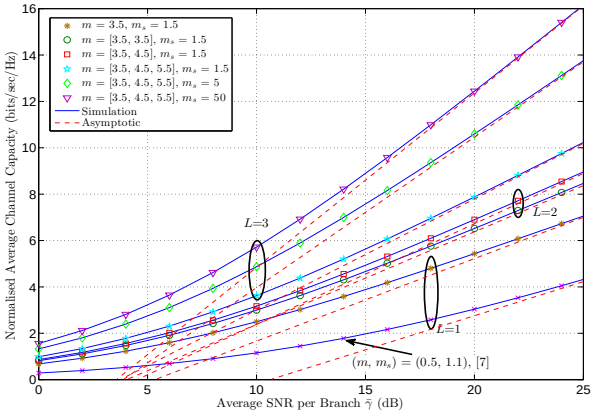

Fig. 2. Normalised ACC of SC scheme with i.n.i.d. branches.

ABEP for $L = 3$ is approximately 82% and 60% less than that for $L = 1$ and $L = 2$ with $m = [3.5, 4.5]$, respectively. Furthermore, for further validations, a comparison between the ABEP of SC and MRC of [8], has been shown in Fig. 1. As expected, the MRC provides less ABEP than the SC but with high implementation complexity. In addition, the result for $L = 1$ of [7] in Fig 2 is obtained by utilising (18). In both figures, the perfect matching between the numerical and the simulation results as well as their asymptotic counterparts at high average SNR can be observed, which confirms the correctness of our derived expressions.

Fig. 3 shows the behaviour of an AUC versus m and m_s and different values of u and L for $\bar{\gamma} = 5$ dB. In this figure, a substantial enhancement in the AUC is occurred when m, m_s, or/and L become large. This is because the increasing in m, m_s, and L would lead to a large number of multipath clusters, less effect of the shadowing, and high received average SNR, respectively. Also, when the parameter u reduces, the value of the AUC increases due to the increasing in both the detection and the false alarm probabilities simultaneously.

VI. Conclusions

In this paper, both the exact and the asymptotic of the PDF and the MGF of the maximum of i.n.i.d. Fisher-Snedecor $\mathcal{F}$ RVs were derived in mathematically tractable closed-form expressions. These statistics were then used to study the performance of the SC diversity reception over i.n.i.d. Fisher-Snedecor $\mathcal{F}$ fading channels. To this end, the exact and the asymptotic expressions of the ABEP, the ACC, and the AUC of an ED were analysed. The diversity order which is proportional to the number of the diversity branches and the parameter m is also provided to validate of our results.

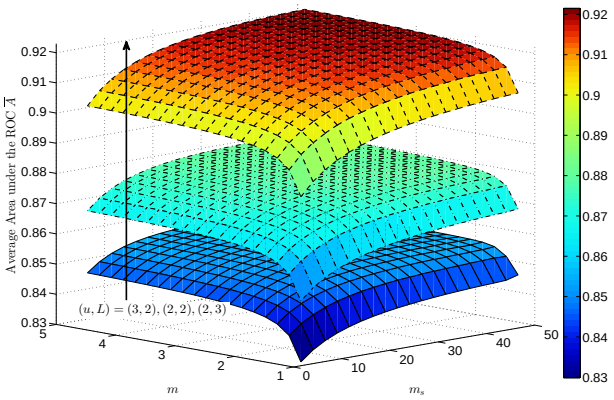

Fig. 3. AUC versus m_s and m and different values of u and L.

References

[1] M. K. Simon and M.-S. Alouini, *Digital Communications over Fading Channels*. New York: Wiley, 2005.
[2] P. S. Bithas, P. T. Mathiopoulos, and S. A. Kotsopoulos, "Diversity reception over generalized-K (K_G) fading channels," *IEEE Trans. Wireless Commun.*, vol. 6, no. 12, pp. 4238-4243, Dec. 2007.
[3] J. Paris, "Statistical characterization of $\kappa - \mu$ shadowed fading," *IEEE Trans. Veh. Technol.*, vol. 63, no. 2, pp. 518-526, Feb. 2014.
[4] H. Al-Hmood, and H. S. Al-Raweshidy, "On the sum and the maximum of non-identically distributed composite $\eta - \mu$/gamma variates using a mixture gamma distribution with applications to diversity receivers," *IEEE Trans. Veh. Technol.*, vol. 65, no. 12, pp. 10048-10052, Dec. 2016.
[5] H. Al-Hmood, *Performance Analysis of Energy Detector over Generalised Wireless Channels in Cognitive Radio*. PhD Thesis, Brunel University London, 2015.
[6] S. K. Yoo *et al.*, "The Fisher-Snedecor $\mathcal{F}$ distribution: A simple and accurate composite fading model," *IEEE Commun. Lett.*, vol. 21, no. 7, pp. 1661-1664, Mar. 2017.
[7] S. K. Yoo *et al.*, "A comprehensive analysis of the achievable channel capacity in $\mathcal{F}$ composite fading channels," *IEEE Access*, vol. 7, pp. 34078-34094, Mar. 2019.
[8] O. S. Badarneh *et al.*, "On the sum of Fisher-Snedecor $\mathcal{F}$ variates and its application to maximal-ratio combining," *IEEE Commun. Lett.*, vol. 7, no. 6, pp. 966-969, Dec. 2018.
[9] S. K. Yoo *et al.*, "Entropy and energy detection-based spectrum sensing over $\mathcal{F}$ composite fading channels," *IEEE Trans. Commun.*, vol. 67, no. 7, pp. 4641-4653, Jul. 2019.
[10] H. Du *et al.*, On the distribution of the ratio of products of Fisher-Snedecor $\mathcal{F}$ random variables and its applications," *IEEE Trans. Veh. Technol.*, vol. 69, no. 2, pp. 1855-1866, Feb. 2020.
[11] I. S. Gradshteyn, and I. M. Ryzhik, *Table of Integrals, Series and Products*, 7th edition. Academic Press Inc., 2007.
[12] A. M. Mathai, R. K. Saxena, and H. J. Haubold, *The H-Function: Theory and Applications.* Springer, 2009.
[13] H. Chergui *et al.*, "Rician K-factor-based analysis of XLOS service probability in 5G outdoor ultra-dense networks," *IEEE Wireless Commun. Lett.*, vol. 8, no. 2, pp. 428-431, Apr. 2018.
[14] O. S. Badarneh and F. S. Almehmadi, "Performance analysis of L-branch maximal ratio combining over generalised $\eta - \mu$ fading channels with imperfect channel estimation," *IET Commun.*, vol. 10, no. 10, pp. 1175-1182, Jul. 2016.
[15] "The Wolfram Functions Website." (Last accessed April 2020).
[16] M. Abramowitz and I. A. Stegun, *Handbook of Mathematical Functions: With Formulas, Graphs, and Mathematical Tables.* New York, NY, USA: Dover, 1965.